3.5 Boundary Physics

3.5.1 Boundary Physics Goals

Boundary physics has both an enabling role and a science role in the NSTX program. The aim of the enabling role is to facilitate access to favorable operational regimes needed for the other elements of the research program. Activities in the enabling role to date have focused on development of conventional wall conditioning techniques, namely helium glow discharge cleaning, boronization, and high temperature bake-out of plasma facing components [1]. These conditioning techniques have enabled routine access to H-mode operation [2,3,4,5], with high stability limits due to low pressure peaking factors [6] and longer pulse length due to high bootstrap current fractions [7,8].

The aim of the science role is to understand the relevant processes governing the boundary plasma and the effect of the boundary plasma on the core. In particular, the boundary plasma research program will have a basic characterization element to test if models developed from conventional aspect ratio

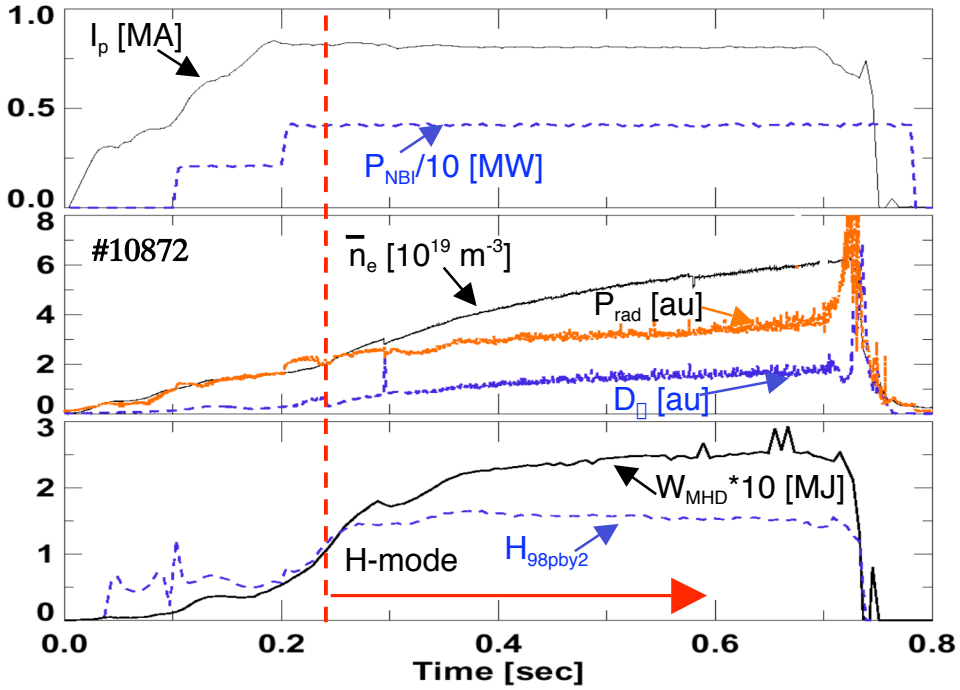

Figure 3.5.1 Long pulse H-mode with density rise

tokamaks fit NSTX observations. In addition, the research will address issues specific to low aspect ratio devices, such as high mirror ratio in the scrape-off layer, high magnetic field line pitch, and short connection lengths compared with conventional aspect ratio machines. In comparison, the research regarding the effect of the boundary plasma on the core is broader, because control of the boundary can facilitate optimization of the core and development of new scenarios.

The boundary physics program goals are closely tied to the IPPA goals. The IPPA goal 3.2.1 states the five year objective (end of FY 2005): "*Make a preliminary assessment of the attractiveness of the ST by assessing high-β_T stability, confinement, self-consistent high bootstrap operation and acceptable heat fluxes for pulse lengths much greater than energy confinement times*". In addition, the implementing approach in 3.2.1.5 gives more detailed guidance on the need for power and particle handling studies, and certain unique features of the ST boundary: *"Study the dispersion of edge heat flux over a range of externally controllable parameters and estimate the plasma facing component requirements under high heating power in the spherical torus magnetic geometry. Determine the ability for managing intense energy and particle fluxes in the edge geometry and for increasing pulse durations significantly beyond the energy confinement time. Most elements of the physics on the edge open field lines are shared between the ST and the tokamak, while the ST introduces stronger variations of the magnetic field strength along the field lines, that are closer to the magnetic mirror. The 'toroidal mirror' configuration also tends to have large flux expansion in the divertor region, likely extending the physics research to new parameter regimes."* In the NSTX program, power and particle handling are the largest elements, followed by studies of the boundary features which differ in ST compared with conventional aspect ratio tokamaks.

The boundary physics program priorities are also partly determined by the needs of next step machines. The main devices affecting this 5-year plan are the NSST, the CTF, and ITER. NSTX is providing a fundamental preview of the challenging boundary physics to be encountered in NSST and CTF, which will be vital to their design specifications. The connection to ITER is in

specific areas where science based models are used to extrapolate to ITER or where ITER-like parameters are achievable within NSTX. In the former case, NSTX can achieve parameters in corners of parameter space not easily accessible to tokamaks, thereby providing an excellent theory testbed. For example, the question of whether the pedestal width depends on either fast or thermal ion gyro-radius will be investigated. In the latter case, NSTX can achieve peak divertor target heat flux in the ITER range of 10 MW/m^2. Each of these projections to future machines will be based on a combination of NSTX data and comparisons with tokamaks and other STs.

Elements of the boundary physics program can be divided into several topics, each of which is discussed below. The first two elements have specific enabling technology goals, as well:

1. particle (fuel and impurity) control

- Goal: maintain steady line density at 3-4 X 10^{19} m^{-3} at 1 MA for current drive

2. power handling and mitigation

- Goal: maintain tile temperature < 1200 ^{0}C with 7 MW NBI and 6 MW RF input

3. H-mode and pedestal physics
4. Edge, SOL divertor and wall conditioning physics

3.5.2 Particle Control and Fueling

a. Background

The advent of gas fueling from the center stack (high-field side, or HFS) in NSTX, the reduction of the intrinsic error field, and the achievement of a 350 deg. C bake-out of all graphite plasma facing components have contributed to enable reproducible access to H-mode transitions and extend the H-mode duration. As a result of these improvements, the H-mode access operational space (i.e. just before the L-H transition) has been increased [5] Typically, the density rises continuously during these long pulse discharges, owing to a combination of good particle

confinement and continual fueling with the high-field side gas injector, neutral beams, and recycling (Figure 3.5.1). The final density approaches 80% of Greenwald scaling ($n_{GW} = I_p/(\pi a^2)$), albeit with no apparent degradation in confinement. During the H-mode phase, the dN_e/dt ($N_e \sim \bar{n}_e * V_{EFIT}$) decays in time similar to the decay of the center stack gas puff rate, suggesting that improved control of the center stack puffing may reduce the dN_e/dt. Also, the edge density continues to increase with time, but the core-density fills in faster, leading to a flat (and sometimes even mildly peaked) density profile at the end of the discharge [4]. This also suggests that the edge source dominates the edge density, and that the core density fills in partly due to inward diffusion from the edge. Typically in these long-pulse H-mode discharges, Z_{eff} in the core is less than 2 and is significantly higher in a narrow region near the plasma edge.

The HFS gas puffing enables a longer H-mode phase than a low-field side (LFS) injector, even when the LFS injector is programmed with identical waveforms [4]. Also, the outboard side gas-fueled discharge exhibited an L-H transition only after the NBI power was increased to 3 MW, suggesting that the L-H power threshold was higher as well. These observations corroborate the premise that fueling plays a strong role in H-mode access in NSTX.

Going forward, density control will be a major effort of the NSTX program, with plans for improved control over sources and sinks (see following section). One of those elements is compact toroid (CT) injection. Because CT injection is a novel, relatively unknown fueling technique, background is given here. The CT injection concept was proposed to achieve deep fueling in tokamaks [9]. A CT injector creates and accelerates the CT by electromagnetic forces. For the CT to penetrate a magnetic field, to first order, the CT kinetic energy density ($\rho V^2/2$) must exceed the target magnetic field energy density ($B^2/2\mu_0$). Initial experiments on the TdeV tokamak have shown that CTs can beneficially fuel an ohmic tokamak discharge without adversely perturbing it [10]. However, because of the small cross-section of the TdeV device, localized core fueling was not achieved. CTs have also been used to trigger H-modes in an ohmic tokamak discharge [11].

Part of the motivation for CT implementation is to fulfill advanced fueling technology needs as laid out by section Section 3.4.1 on Plasma Technologies in the IPPA document: "*The main issues for fueling technologies are to understand and exploit advanced fueling physics (such as high field side launch) and demonstrate the performance (i.e., pellet speeds, density of compact toroids and repetition rates) required to effect adequate control of the density profile shape and high fueling efficiency.*".Eventually, high beta and high bootstrap current fraction discharges in steady state rely on optimized plasma profiles. Under this mode of operation, the fueling system must deposit small amounts of fuel at the desired location so as to compensate for particle losses, while at the same time ensuring that the optimized profiles are not destroyed. CTs also offer the potential of momentum injection in reactor systems where plasma heating is dominated by an isotropic source of fusion alphas, and thus could fulfill reactor fueling needs. Finally, certain ST properties make CT fueling particularly attractive. The lower toroidal field magnitude in a ST relative to a conventional aspect ratio tokamak considerably eases the requirements for CT fueling, while the steep magnetic field gradient in a ST allows for a more precise specification of the CT stopping location.

b. Research Plan, Diagnostics, and Facility Modifications

As discussed above, density control is a near-term need whereas impurity reduction is more of a long-term physics issue. Improved control of the fueling sources is a key element of the research plan. Several staged enhancements will be employed:

1. Additional HFS and LFS gas injectors at different poloidal locations, to determine the optimum trade-off between controllability and H-mode access. The larger the major radius of the injector, the better the control in general. Modeling of the effect of poloidal location of gas injection on H-mode access will be done with UEDGE and DEGAS-2 to determine neutral density profiles, and NCLASS and TRANSP to determine the momentum damping rate. (FY03-FY04)

2. Development of a supersonic gas nozzle, to increase the fueling efficiency and the neutral penetration depth. This effort follows development on several tokamaks. (FY03-FY04)

3. Deuterium pellet injection for deeper and more efficient fueling. We will build on experience from the outboard lithium pellet injector, and add deuterium capability first from the low-field side and possibly the high-field side, if required. Modeling of perturbative pellet injection experiments will be done with TRANSP, TSC and stand-alone pellet ablation codes. (FY05, HFS in FY06)

4. Compact toroid (CT) injection. The single-pulse CT hardware was previously used on the TdeV tokamak and is located at PPPL. Initial preparatory work will be carried out in FY05-06 (see Facilities Section in Chapter 2). A decision on installation will be made at the end of FY06, with initial experiments two years later. (FY08).

Simultaneously with the fueling source control improvements, we will increase the pumping capability through stages, first through advanced wall conditioning techniques for passive pumping and then active pumping options. Note that steps 2, 4, and 5 below represent a staged approach to the introduction of lithium in NSTX.

1. Improved boronization – this includes testing the effectiveness of morning boronization, between shot boronization, boronization with an elevated wall temperature. (FY03-FY04)

2. Lithium conditioning – this begins with pellet injection in the near term, followed by higher yield ablation techniques between or during discharges. (FY03-FY04)

3. Upper divertor lithium film deposition – a between shot lithium film deposition system will be installed in FY04, to coat the upper passive plates and possibly divertor graphite tiles. CDX-U will supply data from a lithium film deposition system on a copper substrate flame-sprayed with Mo, also in FY04. At the end of FY04, a decision on whether to swap out the graphite tiles with CDX-U type prototypes (copper flame-

sprayed with Mo – available for NSTX in FY06) will be made. Additional evaporators will be installed in FY05 for toroidal symmetry. (FY04-06)

4. In-vessel cryogenic condensation pumps – similar to DIII-D and ASDEX-Upgrade, the goal would be active density control during discharges. One option is for active pumping of the outer strike point in the lower divertor. This requires modification of the secondary passive stabilizing plates to create baffles and plenums. The plenum will be designed with analytic models and UEDGE/DEGAS-2 simulations of data. A second option is to install up-down symmetric cryopumps on the horizontal part of the center stack, allowing pumping of high triangularity double-nulls. A decision on which option(s) to implement will be made in FY04 for initial experiments two years later. (FY06)

5. Divertor lithium module – this would address both the active pumping and possibly assist with power handling. The module pumping efficiency is less sensitive to strike point location than a cryopump and thus allows more shape flexibility. In addition, the prospect of a full toroidal module in the lower divertor would allow access to extremely low recycling ($R<0.1$), high temperature regimes. The module design is based on edge modeling of NSTX data, as well as MHD modeling supported by the APEX and ALPS groups. A decision on installation will be made at the end of FY06 for design and installation through FY08, and initial experiments in FY09.

Core fueling experiments and analysis will focus on quantifying the components leading to the observed density rise, i.e. we will identify the fraction of the density rise due to the recycling and NBI sources, and we will also identify the fuel and impurity contributions. This task involves adding visible cameras with D_α filters, and a divertor SPRED XUV system to monitor impurities. The goal is to tomographically reconstruct the poloidal D_α profile, and then map the Thomson Scattering n_e and T_e on flux surfaces to allow a direct calculation of the neutral density and the ionization profile. The edge part of this profile will be simulated with the combination of edge plasma transport codes, such as UEDGE and b2.5, and neutral transport codes, such as DEGAS-

2 and EIRENE, to determine the location of the main recycling surfaces, whether in the divertor or main chamber. In addition, upgrades to the divertor and center stack Langmuir probe array are planned to provide baseline plasma profiles for these modeling codes. Also neutral pressure gauges will be added at several poloidal locations to provide additional data constraints.

Analysis of the particle balance with active pumping will require fast time response pressure gauges near the cryopump, and new diagnostics to measure the stability and uniformity of lithium in the divertor module. Also a mechanism to quantify the particle exhaust with the lithium module will be developed.

Impurity reduction is not a strong near term need but may become one as pulse length and tile heating increase. At present a single-chord VB measurement provides Z_{eff}. A radial profile of Z_{eff} will be obtained from the Thomson Scattering spectrum routinely in FY'04, and the fully stripped carbon density profile will be available routinely from the 51-channel CHERS system in FY'04. The impact of the various source/sink controls listed above on the Z_{eff} and carbon profiles will be examined systematically as the particle control tools become available. If the need arises, our 1-D CCD cameras will be equipped with impurity filters to examine wall impurity source terms. Preparations for SOL/divertor impurity transport studies will be made, but a dedicated program will be considered after completion of the present five-year plan.

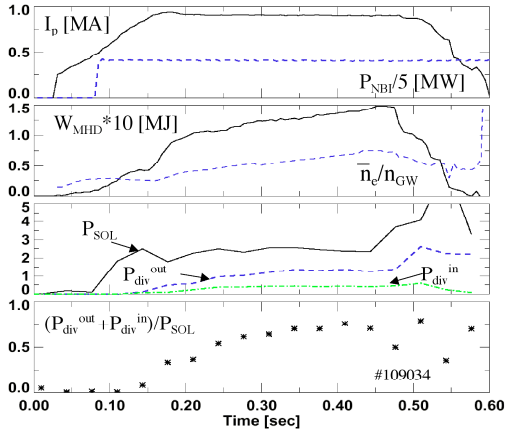

Figure 3.5.2 - Time dependence of power balance. The L-H transition time is indicated by the dashed red line.

3.5.3 Power Handling and Mitigation

a. Background

Edge plasma transport calculations made during the design phase and initial operation of NSTX predicted a peak heat flux in excess of 10 MW/m^2 to the outboard divertor target in the sheath-limited heat

transport regime with little impurity radiation and a range of cross-field transport coefficients. The peak heat flux was shown to increase approximately linearly with power input to the SOL. Thermal design calculations indicated that a peak heat flux above 6-8 MW/m^2 would cause the ATJ graphite tile temperature to rise above the 1200 deg. C administrative limit for a 5 second pulse length. Thus, infrared cameras were installed and heat flux scaling studies were begun recently.

Figure 3.5.2 shows the characteristics of an H-mode lower-single null discharge with 2 MW input power used for power balance analysis. Panel (c) shows the that the outer divertor power (P_{div}^{out}, R > 0.6 m) was about 3 times the inner divertor power (P_{div}^{in}, R < 0.6 m), and that the power flow came to equilibrium by ~ 300ms, a little more than 100ms past the I_p flat-top time. The maximum SOL loss power is given by $P_{SOL} = P_{oh} + P_{NBI} - dW_{EFIT}/dt$, where P_{oh} is the ohmic power, P_{NBI} is the NBI power, and W_{EFIT} is the stored energy computed by EFITD. Note that no charge exchange loss (normally 10%) or core radiation is included (normally 10-20%); hence, the quantity represents an upper bound of the power flow into the SOL. Panel (d) shows that up to 70% of P_{SOL} is observed in the divertor, i.e. the power balance is remarkably good [4].

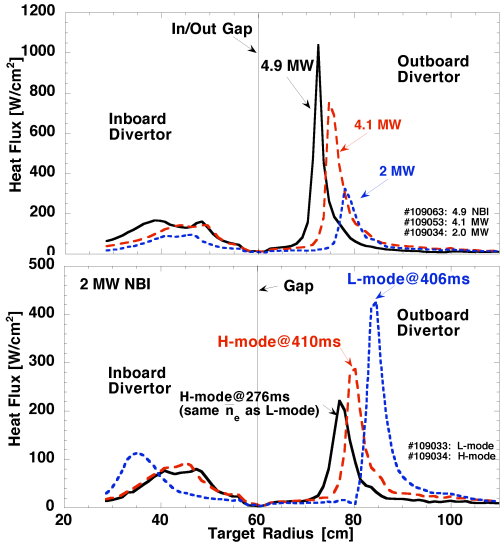

Figure 3.5.3 -Power scaling of heat flux in H-mode and L-mode/H-mode comparison

Calibrated infrared camera measurements (Fig. 3.5.3) of the divertor reveal that the peak flux was 3 times higher on the outboard side at P_{NBI} =2 MW, but increased to 7 times higher at P_{NBI} =5 MW, i.e. the ratio of outer to inner peak heat flux increased with increasing P_{NBI}. Also the outer divertor heat flux profiles were much narrower (full width, half max ~ 2-3 cm) than the inboard ones (full width, half max ~ 10 cm). Finally the outer peak heat flux increased non-linearly with NBI power; the highest measured value in NSTX was ~ 10 MW/m^2, i.e. exceeding

the design limit which would allow a 5 second pulse length. Extrapolation of the temperature rise of the tiles, assuming a constant heat flux and time$^{1/2}$ rise, indicates a pulse length limitation ~ 3 seconds [2].

Figure 3.5.3 (b) compares the heat flux profiles during an L-mode discharge with the same heating power and fueling, and the H-mode discharge in fig. 3.5.2 at a comparable time (red and blue curves) and also a comparable line density (black and blue curves). The L-mode peak heat flux was higher than the H-mode at comparable P_{NBI}, because P_{OH} was higher and dW/dt was lower, i.e. P_{SOL} was effectively higher in the L-mode case. The L-mode profile was marginally broader (2.5 cm vs. 2.2 cm), but it should be noted that the H-mode width was at the limit of spatial resolution of that camera.

Double-null discharges have lower peak heat fluxes than lower-single null, with a preliminary maximum ~ 3 MW/m^2 measured in the lower divertor. While this level appears acceptable for long pulse operation, the heat flux in the upper divertor has not yet been measured.

b. Research Plan, Diagnostics, and Facility Modifications

The maximum input power from NBI and RF heating in the five year plan is 7 MW and 6 MW respectively. Thus the PFC's must be capable of handling up to 13 MW simultaneously for several current relaxation times, i.e. for 0.5-2 sec.

Going forward, heat flux and power balance research will have several elements. The first three elements will provide data for the PFC power handling long pulse upgrade at the end of FY05, which would entail replacement of the divertor ATJ graphite with a suitable PFC material :

1. quantifying the balance between divertor heat flux and core/divertor radiation. This first element requires a more quantitative estimate of the main plasma radiation, which is dominated by the carbon shell at the boundary. (FY04-05)
2. quantitative comparison of single-nulls and double-nulls (FY04-05)
3. heat flux reduction techniques (FY04-06)

4. impact of transient events. e.g. giant ELMs, and reconnection events. (FY05-07)

The present AXUV diode bolometers have a 67% sensitivity drop in the wavelength range characteristic of edge radiation, and cross-calibration with a platinum foil bolometer in the main chamber will be done. Second, the divertor bolometer will be augmented to provide a profile of divertor radiation. Investigating the trade-offs between radiation and heat flux as a function of control parameters will be a main focus. High toroidal peaking factors of peak heat flux would reduce the maximum allowed average heat flux; thus, an assessment of the toroidal peaking factors will be done.

Because single-nulls are used in pulse length studies and double-nulls are used in beta limit and performance studies, a quantitative comparison of the heat flux distributions in each configuration will be done. Included in this task is the assessment of the up/down power balance in double-nulls. Experiments on conventional aspect ratio tokamaks [12] and the MAST device [13] have indicated the importance of the magnetic flux balance in affecting the up/down split, and similar studies will be conducted in NSTX. Finally a set of experiments to measure the change in power flux distributions as the inner-wall gap is reduced will be conducted, to determine if the center stack can be used to reduce the divertor heat flux without excessive heating and while maintaining good performance. Additional IR cameras will be installed for this task.

The level of emphasis on heat flux reduction techniques will depend partly on if the temperature rise of the tiles restricts pulse length. If the central electron temperatures remain below ~ 2 keV, the current diffusion time will remain below 500 msec, and NSTX will be able to accomplish programmatic goals without the need for heat flux mitigation. An approximate doubling of $\langle T_e \rangle$ from the scenarios discussed in chapter 4 would be required to increase the current diffusion time to several seconds, in which case the temperature rise of the tiles may restrict pulse length in lower-single nulls. In any case, heat flux reduction via deuterium gas puffing, impurity injection and outer divertor biasing will be studied in support of physics needs of an ST component test

facility. In addition, heat flux reduction will be studied to confirm the physics of detachment in an ST, discussed in the divertor physics section. Understanding of the steady power flow and heat flux reduction techniques will be attained through UEDGE/DEGAS-2 modeling. These data and analysis will determine if PFC upgrades are required to handle the heat loads as the pulse length is extended (decision point – end of FY05).

Finally, the heat flux studies to date and mentioned above are based on quasi-steady thermal response measured by IR cameras with conventional 30-60 Hz framing rate. An important set of experiments concerns tile response to giant ELMs and reconnection events. ELMs as large as $\Delta W/W_0 \sim 25\%$ (where W_0 = plasma stored energy before ELM) have been measured on NSTX, and reconnection events caused by MHD activity or during plasma current ramp down need to be investigated to support future, larger ST designs and also design of the Lithium module for pumping within NSTX. The giant ELMs are triggered in low recycling conditions in lower-single null discharges and could become the norm when active density control is implemented. The heat flux associated with these off-normal events will be measured with a fast IR camera with framing rates in the 30 – 100 kHz range.

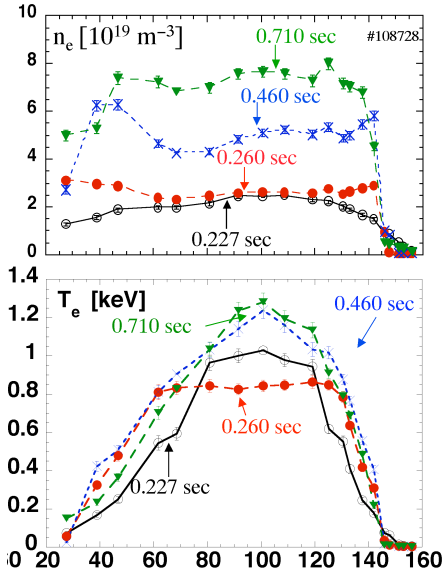

Figure 3.5.4- Density and electron temperature evolution following an L-H transition

3.5.4 H-mode transition, pedestal, and ELM physics

a. Background

This area overlaps significantly with the transport section, and comprises three linked subject areas: transition, pedestal and ELM physics. The plans related to L-H transition physics, e.g. in

terms of power threshold, E X B shear, fast ion event triggers, etc. are discussed in the transport section.

H-mode pedestal physics and ELMs are clearly linked: it is generally believed that the steep gradients in the pedestal lead to relaxation phenomena which are manifest as ELMs. As reported previously [14], the density profile becomes hollow just after the L-H transition, forming 'ears' on both the inboard and outboard sides (Fig. 3.5.4). The density profile flattens [4] in the longer H-mode discharges after 300-500ms. From Thomson Scattering and reflectometer data, the density pedestal full width can be estimated as ~ 3-4 cm, i.e. in the range of the largest widths reported by the DIII-D tokamak. Mapped into normalized toroidal flux space, the pedestal extends in as far as $\Psi_{NORM} \sim 0.8$, much deeper than DIII-D's pedestal which extends to $\Psi_{NORM} \sim 0.95$. Also of note is that the density pedestal is routinely higher on the inboard side than the outboard, as also observed on the MAST device [13]. Evolution of the temperature profile is also shown in Fig. 3.5.4. First, the temperature pedestal is rather modest, reaching a maximum of 400 eV, limited by present spatial resolution of Thomson Scattering. Second, it appears that the core temperature rides up and down on the pedestal, as opposed to experiencing a proportional increase in the core gradient.

A wide range of ELM behavior has already been observed on NSTX, with some interesting differences as compared with conventional aspect ratio tokamaks [5]. Figure 3.5.5 shows the three most prevalent D_α behavior: either ELM-free (or perhaps very rapid, small ELMs) in panel (a), giant ELMs dumping up to 25% of stored energy in panel (b), and 'regular' ELMs in panel (c). Panels (a) and (b) are both obtained in low $\kappa \sim 0.4$ lower-single null discharges. The larger ELMs in panel (b) are obtained either with reduced gas fueling just above the locked mode threshold or on the first fiducial discharge in the morning of an experiment, which has lower recycling than subsequent discharges. The 'regular' ELMs in panel (c) are obtained in high κ (~ 0.6-0.8) double-null discharges. Preliminary analysis shows that the amplitude (frequency) of these ELMs decreased (increased) with input power up to a point, i.e. a characteristic of Type I ELMs in conventional aspect ratio tokamaks.

b. Research Plan, Diagnostics, and Facility Modifications

Going forward, the program in this area will progress from qualitative pedestal and ELM characterization (FY04-05) to quantitative theory comparisons (FY06-08) as the relevant edge diagnostics become available.

Experiments will be carried to determine the control parameters (e.g. collisionality and neutral penetration length) of the pedestal density height and width, including the upper and lower limits and relevant density-limiting processes. Also the role of rotation and in/out magnetic field strength differences on determining the in/out pedestal heights will be investigated. Experiments to correlate the stiff electron transport observed [15] in NSTX with pedestal parameter changes will be conducted. Finally we will examine scaling of the global confinement and stored energy with pressure pedestal height. These scalings of the pedestal height, width, and maximum gradient are crucial to reactor design. With its low aspect ratio and toroidal field, NSTX (and also MAST) will provide a unique data set to the international pedestal working group, which will test predictive models of the pedestal. Aspects of pedestal scaling will be tested both with analytic models and more comprehensive gyrokinetic simulations (e.g. the GYRO code). Pedestal asymmetries from the high-field side and low-field side will be studied with analytic models developed through additional or future collaborations.

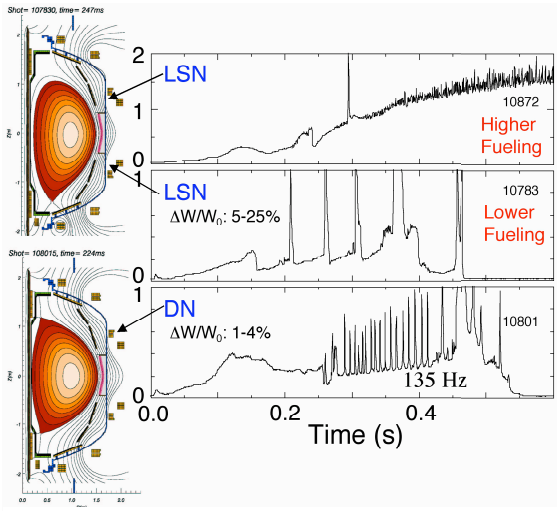

Figure 3.5.5- variety of ELM sizes and types observed in NSTX

On the surface, certain aspects of the ELM observations in NSTX are contrary to conventional aspect ratio tokamaks, where the largest ELMs are often observed in higher □, higher performance double-null discharges. Basic ELM research will include a measurement of the ELM amplitude and frequency dependence on plasma and external parameters. While our initial

characterization has focused on $\Delta W/W_0$, the fraction of pedestal energy lost per ELM ($\Delta W/W_{ped}$) is the more relevant metric for future studies. In addition, ELM research will include experiments aimed at the causality of the observed differences in double-null and single-null configurations. Experiments will also be carried out to test recent models which consider the ELM as a de-stabilization of peeling and/or ballooning modes. Finally, optimization of ELMs for density and impurity control will also be explored. Simulations of the instabilities responsible for ELMs will be done (with e.g. the ELITE code) after sufficient spatial resolution is obtained on edge diagnostics.

Quantitative comparison to pedestal, ELM, and L-H transition theories will be enabled by increased spatial and temporal resolution of the Thomson Scattering diagnostic (FY04, FY06) and improved time resolution (down to 1 msec in FY07) of the CHERs system. In addition, edge current density measurements with MSE will be available in FY06. Also, a helium line ratio technique to obtain fast time scale n_e and T_e data at the outer edge will be implemented in FY06.

3.5.5 Edge, SOL divertor and wall physics

a. Background

This area covers two topics: 1) the nature of edge and divertor transport, and 2) development and evaluation of wall conditioning techniques. The classical picture [16] of divertor transport includes parallel transport on open-field lines and anomalous diffusive and/or convective transport across the field lines. In this picture, three regimes of particle and energy transport emerge: 1) a low recycling, high heat flux regime with the temperature drop occurring at the sheath; 2) a high recycling, lower heat flux regime with temperature gradients along the field lines; and 3) a detached regime in which radiation and convection dominate. In this last regime, the plasma temperature falls low enough for volumetric recombination to extinguish a portion of the plasma before striking the target; high neutral pressure is thought to play a key role. From

existing data, it is likely that both the sheath-limited and high-recycling regimes have been observed in NSTX.

In addition, the paradigm of steady (but anomalous) cross-field transport may be inapplicable to NSTX (as also discussed in the transport section of this document). Recent experiments [17,18] on NSTX and C-MOD with the gas-puff imaging (GPI) diagnostic have indicated the existence of localized density perturbations which propagate both poloidally and radially. Fig. 3.5.6 shows the GPI diagnostic view and two images: 1) a quiescent H-mode image, obtained by puffing helium gas into a deuterium plasma at the outer midplane; and 2) a non-quiescent H-mode with clear structure. The smooth, curved light emission from the quiescent H-mode follows the local field line pitch near the separatrix. The bright region in the non-quiescent H-mode is indicative mainly of a local density increase. These local density perturbations can often be seen propagating radially and poloidally, sometimes to the RF antenna. These intermittent structures are common in L-mode but also exist in H-modes. The existence of intermittent radial transport in NSTX has been recently confirmed with the UCSD mid-plane reciprocating probe measurements.

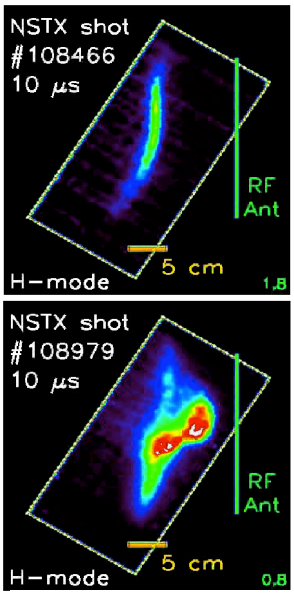

Figure 3.5.6 - gas puff images of a quiescent and non-quiescent H-modes

b. Research Plan, Diagnostics, and Facility Modifications

Going forward, the program time line in this area entails:

1. Determine SOL/divertor transport regimes (FY04-08)
2. Examine ST unique edge physics effects (FY05-08)
3. Investigate the nature of edge transport in NSTX (FY04-08)
4. Develop and investigate wall conditioning techniques (FY04-08)

Experiments will be conducted to document the presence or absence of the aforementioned divertor regimes, and detailed comparisons will be made with edge plasma transport codes, such as UEDGE, and neutral transport codes, such as DEGAS-2. For example, plasma detachment has been predicted to be more difficult to obtain in NSTX due to the short connection length. Quantitative comparisons with these models will be facilitated by the installation of an improved spatial resolution divertor Langmuir probe array in FY05-06, and the installation of fast time response divertor neutral pressure gauges in FY04-05. In addition, a divertor Thomson scattering system will provide local n_e and T_e measurements in FY07, and a divertor imaging spectrometer will provide flow velocity in FY06. It is anticipated that some of the new diagnostics in this section 3.5.5 will be implemented and operated through existing or new collaborations.

Certain effects specific to low aspect ratio may alter the classical divertor picture in NSTX. For example, the total magnetic field varies by up to a factor of 4 from the outer mid-plane to the outer target in high β plasmas. This variation in |B| leads to a mirror force on scrape-off layer ions, adding the possibility of separate parallel and perpendicular temperatures. Calculation of this effect is being implemented in the UEDGE code, and diagnostics to measure the asymmetry of the temperature (e.g. energy extract analyzers in FY07) will be installed to test UEDGE predictions. In addition, the ratio of the magnetic field at the inner to outer strike points can be considerable, leading to important differences in the E X B drift pattern near the separatrix through the private flux region. A divertor reciprocating probe will be installed in FY05 to measure the importance of these flows. Simulation of these ST specific effects will also be done with SOL kinetic transport codes, which will be developed through collaborations. Results of these kinetic code calculations will be implemented as kinetic adjustments to the UEDGE fluid transport model.

In the area of cross-field transport, future experiments will be conducted to fully characterize the intermittent phenomena discussed above; the results will be compared with boundary turbulence codes, such as BOUT. The effects of these bursts on mid-plane plasma decay lengths will be measured and compared with cross-field transport models. In addition, some effort will be made

to compare the mid-plane turbulence with divertor turbulence, by using a fast-framing divertor camera (FY04) and the new reciprocating probe (FY05), mentioned above, which will plunge into the X-point region. Finally additional reflectometer channels (FIRtip) will allow measurement of density fluctuations ($\tilde{n}_e / n_e$) at the plasma edge in FY05.

Evaluation and improvement of wall conditioning techniques will continue. Some of these techniques were described in the section on particle control. Upgrades to a quartz crystal deposition monitor will allow correlation of wall deposition and erosion with plasma operating conditions (FY04). In addition, wall coupons will be periodically examined via standard surface analysis techniques to evaluate the film composition from various conditioning techniques and integral wall erosion due to fast charge exchange neutrals. Finally, a divertor materials probe similar to the DiMES probe on DIII-D will be installed for materials testing in FY07.

3.5.6 Time line

The time line below lays out aspects of the boundary physics program. The diagnostic boxes are aligned with the time range when the first quantitative data could be obtained.

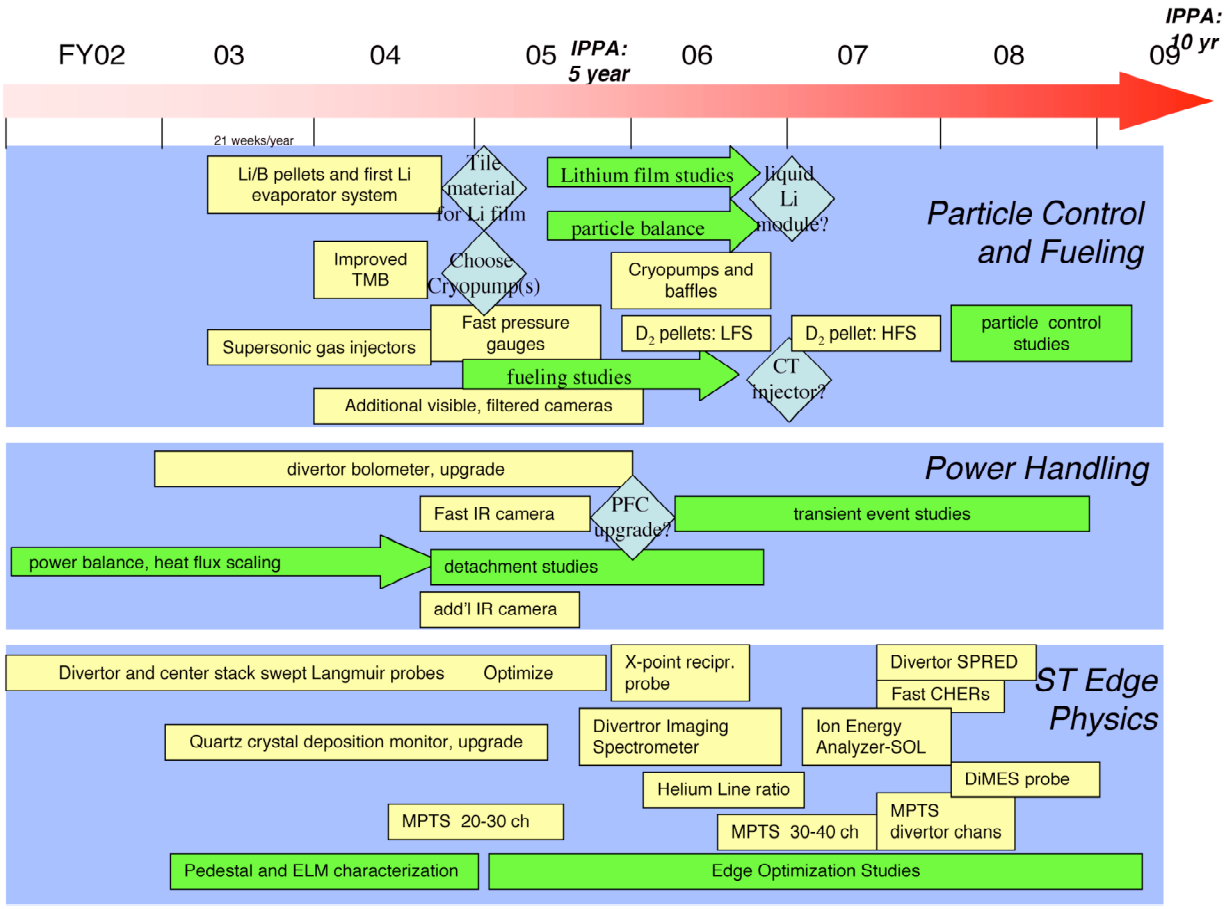

References:

[1] Kugel, H.W. *et. al., J. Nucl. Mater*. **313-316** (2003) 187.

[2] Maingi, R. *et. al., Plasma Phys. Contr. Fusion* **45** (2003) 657.

[3] Synakowski, E.J. *et. al.,* submitted to *Nucl. Fusion*.

[4] Maingi, R., *et. al.,* submitted to *Nucl. Fusion*.

[5] Bush, C.E., *et. al., Phys. Plasma* **10** (2003) 1755.

[6] Sabbagh, S.A. *et. al.,* submitted to *Nucl. Fusion*.

[7] Menard, J..E. *et. al., Nucl. Fusion* **43** (2003) 330.

[8] Gates, D.A., *et. al., Phys. Plasma* **10** (2003) 1659.

[9] L.J. Perkins, *et. al., Nucl.Fusion* **28** (1988)1365; P.B. Parks, *Phys. Rev. Letts.* **61** (1988) 1364.

[10] R. Raman *et. al., Nucl. Fusion*, **37** (1997) 967.

[11] C. Xiao, *et. al.,* "Compact Torus Injection Experiments in the STOR-M Tokamak", *Proc. of 4th Symp. on Current Trends in International Fusion Research:Review and Assessment* (Washington D.C., March 12-16, 2001, in print)

[12] Lasnier, C.J. *et. al., Nucl. Fusion* **38** (1998) 1225.

[13] Carolan, P, *et. al.,* submitted to *Nucl. Fusion*

[14] Maingi, R, *et. al., Phys. Rev. Letts.* **88** (2002) 035003.

[15] LeBlanc, B.P. *et. al.,* submitted to *Nucl. Fusion*

[16] Mahdavi, M.A., *et. al., Phys. Rev. Letts*. **47** (1981) 1602.

[17] Zweben, S.J. *et. al., Phys. Plasma* **9** (2002) 1981.

[18] Terry, J., *et. al.,* submitted to *Nucl. Fusion*